Title: Carboxymethylated Bacterial Cellulose: an environmentally friendly adsorbent for lead removal from water

Authors: Ezequiel Rossi, Úrsula Montoya Rojo, Patricia Cerrutti, María Laura Foresti, María Inés Errea

PII: S2213-3437(18)30664-X
DOI: https://doi.org/10.1016/j.jece.2018.10.055
Reference: JECE 2741

To appear in:

Received date: 6-9-2018
Revised date: 24-10-2018
Accepted date: 25-10-2018

Please cite this article as: Rossi E, Rojo ÚM, Cerrutti P, Foresti ML, Errea MI, Carboxymethylated Bacterial Cellulose: an environmentally friendly adsorbent for lead removal from water, *Journal of Environmental Chemical Engineering* (2018), https://doi.org/10.1016/j.jece.2018.10.055

Carboxymethylated Bacterial Cellulose: an environmentally friendly adsorbent for lead removal from water

Ezequiel Rossi[a,b], Úrsula Montoya Rojo[b,c], Patricia Cerrutti[c,d], María Laura Foresti[b, c] and María Inés Errea[a*]

[(a)] Instituto Tecnológico de Buenos Aires (ITBA), Buenos Aires, Argentina.

[(b)] Consejo Nacional de Investigaciones Científicas y Técnicas (CONICET), Argentina.

[(c)] Grupo de Biotecnología y Biosíntesis. Instituto de Tecnología en Polímeros y Nanotecnología (ITPN-UBA-CONICET), Facultad de Ingeniería, Universidad de Buenos Aires, Argentina.

[(d)] Departamento de Ingeniería Química, Facultad de Ingeniería, Universidad de Buenos Aires, Argentina.

[*]*Corresponding author: Tel/Fax: 54-11-2150-4800.*

E-mail address: merrea@itba.edu.ar

Graphical abstract

Highlights

- Insoluble Carboxymethylated Bacterial Cellulose (CMBC) was synthesized.

- CMBC exhibited good lead adsorption capacity in both, batch and column experiments.
- CMBC Hydroxyl groups improved its adsorption capacity.
- CMBC lifetime was over 50 adsorption/desorption cycles.

Abstract

Carboxymethylated bacterial cellulose (CMBC) was synthesized under controlled reaction condition to provide a material with a degree of substitution (DS) that guarantees that the characteristic water insolubility of cellulose is retained (DS=0.17). The CMBC synthesized was fully characterized by conductometric titration, infrared spectroscopy, scanning electron microscopy, energy-dispersive X-ray spectroscopy, thermogravimetric analysis and solubility assays. The suitability of the produced CMBC for lead removal from water was evaluated. Experimental isotherm data were fitted to different models of sorption isotherms: Langmuir, Freundlich, Dubinin-Radushkevich, and Frumkin, with Langmuir equation resulting in the best fit. Kinetic data were also adjusted to pseudo-first-order and pseudo-second-order models and results undoubtedly showed that the pseudo-second-order kinetic equation was the one that most appropriately described the lead adsorption of CMBC, indicating that lead is adsorbed on CMBC predominantly by chemical interaction. The breakthrough curve was fitted to different models: Bohart-Adams, Clark and Modified Dose-Response, being the Bohart-Adams equation the one that gave the best fit. Desorption studies were carried out in order to know the technical feasibility of the reuse of CMBC. Almost 96 % of the retained lead was eluted in just 20 mL, and the CMBC lifetime was over 50 adsorption/desorption cycles. Overall, results obtained suggest that the CMBC herein synthesized may result in an alternative economic and environmentally friendly lead adsorbent for water treatment.

Keywords: Lead; Carboxymethylated bacterial cellulose; Adsorption; Ion exchanger; Breakthrough curve

1. INTRODUCTION

One of the major concerns associated with the continuous increase in world population is the availability, in the near future, of natural resources that ensure the sustainability of life. In particular, in the case of freshwater, together with its shortage, its deterioration by anthropogenic factors needs to be considered. Among the most common water pollutants, heavy metals are highly disturbing due to their non-biodegradability and their high toxicity [1]. For instance, lead (Pb) is a potent neurotoxin that has no biological role, and its ions (Pb II) may cause critical diseases in human beings, including cancer [2–4]. Lead can be found in aqueous systems mainly as a consequence of lixiviation of mining areas, but also because of industrial effluents. The US Environmental Protection Agency (EPA) has set the maximum contaminant level (MCL) for the lead at 15 ppb for drinking water [5]. Thus, many researchers invest their efforts in the development of systems that allow the elimination of lead from water to levels as low as those established by EPA. Precipitation, solvent extraction, membrane filtration, reverse osmosis, ion exchange, flotation, coagulation-flocculation, and adsorption are the strategies commonly investigated [1,6,7]. Among all those methods, adsorption is particularly attractive because of its high efficiency, low cost, easy handling and high availability of different adsorbents, being those derived from renewable biomass especially attractive. Biopolymers, like chitosan, alginate, and cellulose, are particularly advantageous because of their cost-effectiveness, their sustainable long-term availability and their harmlessness to the ecosystem [8–12].

Particularly, many cellulose-containing materials and cellulose derivatives have been reported as useful for the adsorption of heavy metals [9,13–16]. Both, the natural abundance of cellulose, and the possibility of obtaining it not only from pulps derived from wood but also from a number of alternative abundant and underutilized cheaper

cellulose sources such as annual fiber crops, agricultural residues, and wild plants; make this polysaccharide very attractive as raw material for the development of adsorption systems. On the other hand, the isolation of cellulose from plant sources implies the use of reagents that can have a negative environmental impact [17]. Conversely, bacterial cellulose (BC) has the same molecular formula as plant cellulose, but it has the advantage of being produced free of lignin, hemicelluloses and pectin; thus avoiding the need for chemical treatments devoted to the removal of these compounds prior to cellulose derivatization. Moreover, BC is recognized for other distinguishing properties such as a high degree of polymerization, crystallinity and loading capacity; and a unique nanofibrillar structure which determines its extraordinary physical and mechanical properties. Furthermore, the possibility of designing the shape and porosity of the membranes obtained in static culture is another very attractive feature of BC, all encouraging its use in traditional plant-derived cellulose applications.

In addition to the advantages described before, the hydroxyl groups of cellulose can be reacted with different chemicals to provide derivatives with a broad range of properties and therefore with a broad range of potential applications. For instance, cellulose can be carboxymethylated to give carboxymethyl cellulose (CMC), a well-known ionic polysaccharide useful as a cation exchanger. Taking into account that Pb (II) exists as a positive ion in aqueous systems, CMC could be an option to purify lead-contaminated water [18].

Water solubility of CMC depends on its degree of substitution (DS), defined as the average number of hydroxyl groups substituted with carboxymethyl groups per anhydroglucose unit (AGU). Previously, some of us reported a systematic study on the manipulation of reaction conditions to produce carboxymethylated BC (CMBC) with tailored DS [17]. Based on our previous experience, insoluble carboxymethyl cellulose

to be used in lead removal was herein synthesized. The new material was fully characterized by infrared spectroscopy (FT-IR), scanning electron microscopy (SEM), energy-dispersive X-ray spectroscopy (EDS), thermogravimetric analysis (TGA) and solubility assays. Besides, in order to determine the CMBC effectiveness for removing Pb (II) from water, adsorption studies were carried out. Adsorption isotherm models (Langmuir, Freundlich, Dubinin–Radushkevich, and Frunkin) were used to elucidate possible adsorption mechanisms [18–20]. The effects of operational parameters (pH, ionic strength, and contact time) on the adsorption capacity were also investigated. Furthermore, to analyze the economic feasibility of the use of CMBC for the proposed application, the maximum number of regeneration cycles was studied. In order to predict the process scale-up, the breakthrough curve was also constructed.

2. EXPERIMENTAL

2.1 Instrumentation and reagents

BC culture medium was formulated using glycerol (Sintorgan), disodium phosphate.12 H_2O, citric acid (Biopack), meat peptone and yeast extract (Britania). Sodium monochloroacetate (NaMCA) was purchased from Aldrich Chemical Company and used as received. All other reagents required for BC carboxymethylation and recovery (isopropanol, sodium hydroxide, acetic acid, methanol) were of analytical grade and used as received.

Aqueous solutions of Pb (II) were prepared from solid $Pb(NO_3)_2$ p.a. (Merck). Solutions were prepared with ultrapure water (18 MΩ quality). Lead concentration was determined on an air-acetylene flame type atomic absorption spectrometer (FAAS) (Model iCE 3000, Thermo Scientific). Pb (II) standard solutions for the FAAS analyses were prepared from 1000 mg L^{-1} Pb standard solution (Merck).

2.2 Production of BC

BC was produced in static culture using a *Gluconacetobacterxylinus* strain under optimized conditions previously described [21]. Briefly, inocula of *G. xylinus* were cultured at 28ºC for 72 h under static conditions in 250 mL erlenmeyer flasks containing 50 mL of Hestrin and Schramm (HS) medium [22]. After that, the inocula (10% v/v) were transferred to 250 mL erlenmeyer flasks containing 50 mL of modified HS fermentation medium (glucose was replaced by glycerol) and incubated at 28 ºC for 15 days under static conditions. The produced BC pellicles were then harvested, thoroughly rinsed with distilled water to remove the culture medium, treated with KOH solution (2 % w/v) during 1h at 90°C to eliminate the bacterial cells, again washed with distilled water till neutral pH was achieved, and finally homogenized three times (5 min each).

2.3 Carboxymethylation procedure

The BC suspension (1 g dry weight, 6.2 mmol anhydroglucose units) was solvent-exchanged from water to isopropanol (twice, 70 mL) to remove water without BC hornification. Carboxymethylation of BC was carried out as described previously [17]. Briefly, the suspension of BC in isopropanol was stirred at 300 rpm for 10 min. Then, NaOH solution (35 % w/v; NaOH:AGU molar ratio 3:1) was added dropwise and the reaction mixture was stirred for 1 h at 30°C. Finally, sodium monochloroacetate (NaMCA:AGU molar ratio 1:1) was added and the mixture was kept at 55°C for 2 h with continuous stirring.

The crude product was filtered off, the residue was re-suspended in methanol (75 mL) and neutralized with acetic acid. The suspension was filtered, the residue was washed with ethanol (70 % v/v), dried at 60°C overnight and finally ground to powder.

2.4 Characterization of CMBC

Samples were analyzed for degree of substitution (DS), morphology, elemental composition, chemical structure, crystallinity, thermal stability and solubility in water. The degree of substitution was determined by conductometric titration as described elsewhere [23]. The morphology of native BC, alkali-treated BC and CMBC samples was studied in a scanning electron microscope Zeiss Supra 40 with field emission gun operated at 3 kV. CMBC samples were also analyzed for elemental composition after lead adsorption assays and after the regeneration treatment in a Phenom World ProX scanning electron microscope working at 15 kV acceleration voltage and equipped with a Silicon Drift Detector for EDS analysis. *FT-IR* spectra of ground native and CMBC samples were acquired on an IR Affinity-1 Shimadzu Fourier Transform Infrared Spectrophotometer in absorbance mode. The carefully dried samples (12.5 mg, 110 ºC, overnight) and KBr (dried 110°C, overnight) were blended in the ratio 1:20 and dried at 110 °C overnight. Spectra were recorded in the 650-4000 cm^{-1} range with a spectral resolution of 4 cm^{-1}, and normalized against the 1168 cm^{-1} band, which is associated with the asymmetric stretching vibration mode of the cellulose glycosidic linkage [24]. The structure of ground BC and CMBC samples was analyzed with a Rigaku D/Max-C automated wide-angle powder X-ray diffractometer operated at 40 kV and 30 mA, with Cu/Kα radiation (λ= 0.154 nm). X-ray diffraction diagrams were recorded in a 2θ angle range of 10–40° with a scan rate of 0.6°/min and a step size of 0.02°. Thermogravimetric analysis of preconditioned BC and CMBC samples (5 mg, 110 ºC, 1 h) was conducted in a TGA-50 Shimadzu instrument. Samples were heated from 25°C to 850°C at a constant heating rate of 10 °C min^{-1} under a nitrogen atmosphere (30 mL min^{-1}, 2 kg cm^{-2}). Finally, to study the water solubility of CMBC, a film was made by drying the sample between glasses at 110°C for 2 h. The film obtained was weighed before being placed in a beaker with 50 mL of distilled water under static conditions for

24 h. Within this interval of time, the film was periodically removed from water, visually inspected, dried at 110°C for 1 h and finally weighed.

2.5 Batch Adsorption Studies

2.5.1 Adsorption kinetics

Alkali-treated BC or CMBC (50 mg) were suspended in 100 mL of lead solution (100 mg L^{-1}) at pH 7 and the mixtures were stirred at 400 rpm at different temperatures (25, 35 and 45°C). Samples were taken from each suspension at different times and lead concentration was determined by FAAS. As it was expected, BC showed a maximum lead adsorption capacity almost ten times lower than CMBC.

2.5.2 Effect of pH

The effect of pH on the adsorption of lead was studied in a pH range of 2.5-7.0 at 25 °C. 25 mL of an aqueous lead solution (100 mg L^{-1}) was shaken in presence of 25 mg of CMBC at 400 rpm for 2 h. The pH of the solutions was adjusted using HCl (0.01 M) or NaOH (0.01M). After filtration, lead concentration was determined by FAAS.

2.5.3 Effect of ionic strength

The effect of ionic strength on the adsorption of lead was studied using NaCl solutions of concentrations ranging from 1 to 100 mM. 25 mL of aqueous lead solution (100 mg L^{-1}) at pH 7 was shaken with 25 mg of CMBC at 400 rpm and 25°C for 2 h. After filtration, lead concentration was determined by FAAS.

2.5.4 Adsorption isotherms

The adsorption isotherm experiments were carried out by adding a fixed amount of CMBC (25 mg) to 25 mL of lead solution (50-150 mg L^{-1}) at pH 7 at different temperatures (25, 35 and 45°C). The mixtures were stirred at 400 rpm for 2 h. After filtration, lead concentration was determined by FAAS.

2.6 Column experiments

Column experiments were carried out using an acrylic column (I.D. 6 mm, L. 22 mm) filled with CMBC (50 mg) and connected to a peristaltic pump by tygon tubes. In all cases, the flow rate was set at 2.5 mL min^{-1}.

2.6.1 Breakthrough curve

Aqueous lead solution (7 mg L^{-1}) at pH 7 was sent into the column. The effluent was collected in 10 mL fractions and the concentration of lead in all fractions was determined by FAAS.

2.6.2 Desorption studies and regeneration cycles

Metal desorption was carried out with aqueous HCl solution (6 mM, 100 mL, pH 2.2). The effluent was collected in 1 mL fractions and the concentration of lead in all fractions was determined by FAAS.

After lead elution, the CMBC was conditioned with an NaOH aqueous solution (10 mM, 5 mL) and washed with water until pH 7 prior to use again to study the regeneration cycles. The procedure was repeated 50 times.

3. RESULTS AND DISCUSSION

3.1 Characterization of CMBC

The DS of CMBC -determined by conductometric titration- was 0.17, and the insolubility of the sample was confirmed by no significant change in the sample's weight after being immersed in water during 24 h. Comparison of *FT-IR* spectra of BC and CMBC samples also provided evidence of etherification (Fig. 1). In the CMBC spectrum, apart from the typical bands of cellulose [25], the band characteristic of the stretching vibration of the carboxylate groups at 1607 cm^{-1} was observed, confirming that carboxymethylation had occurred.

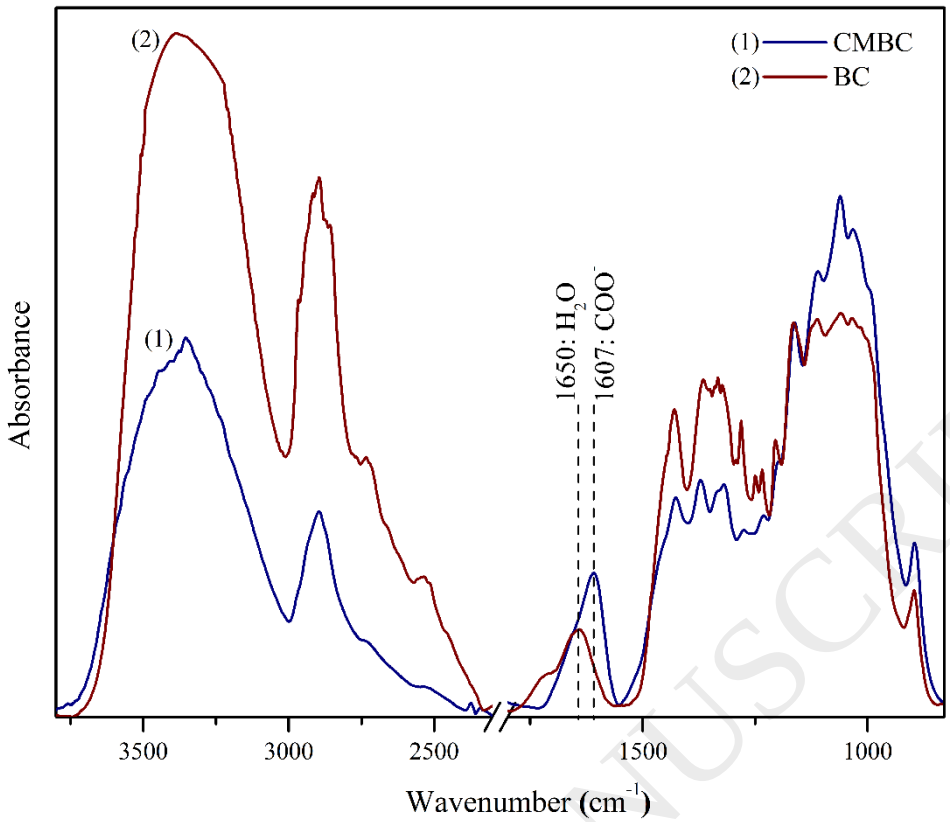

Fig.1 *FT-IR* spectra of BC and CMBC

The thermal stability of BC and CMBC is illustrated in Figure 2. Heating of BC in nitrogen atmosphere resulted in a first weight loss event between room temperature and ≈ 140 °C assignable to the sample's dehydration. The following weight loss exhibited in BC thermogram corresponded to BC decomposition, and it was characterized by T_{onset} and T_{max} values of 304 °C and 376 °C, respectively. T_{onset} was calculated as the temperature of 5 wt.% weight loss after moisture removal. T_{max} stands for the point of greatest rate of change on the weight loss curve. CMBC thermogram also showed a dehydration step, which was more significant in this case due to the increased hydrophilicity of the CMBC sample resulting from derivatization. Two clearly distinguished decomposition events of different relevance followed dehydration. The first thermal decomposition stage exhibited a T_{onset} of 257 °C and a T_{max} of 320 °C. This stage is associated with the thermal decomposition of unmodified BC portions with

reduced crystallinity resulting from carboxymethylation [17]. Significant reduction of the thermal stability of cellulose and nanocellulose upon carboxymethylation has been previously reported [26,27]. The second decomposition event shown in CMBC thermogram occurred at temperatures higher than 600 °C. The correspondence of this event with the number of carboxymethyl groups present in the sample has been previously demonstrated by some of us [17]. Dodi et al. (2011) also observed a high-temperature decomposition event in carboxymethylated guar gum samples, which was attributed to carboxymethyl groups decomposition [28].

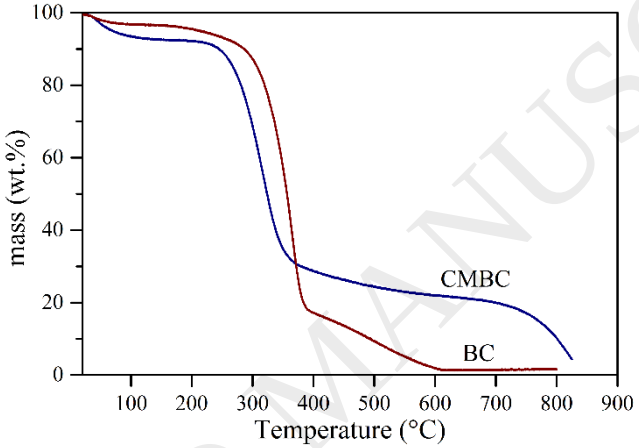

Fig. 2 TGA analysis of BC and CMBC

Figure 3 collects the SEM images of neat BC, alkalinized BC and CMBC samples after oven-drying followed by grinding. As it is shown, although retaining its fibrous character, oven-dried CMBC evidenced significant aggregation of BC nanoribbons, a phenomenon also observed in the alkalinized non-etherified sample.

The presence of Pb in CMBC samples was analyzed by EDS, before and after regeneration with HCl (6 mM) (Fig. 4). After adsorption assay, Pb could be detected in the corresponding element distribution (4-14 weight %, depending on the sample region analyzed), whereas after regeneration no Pb signal was identified.

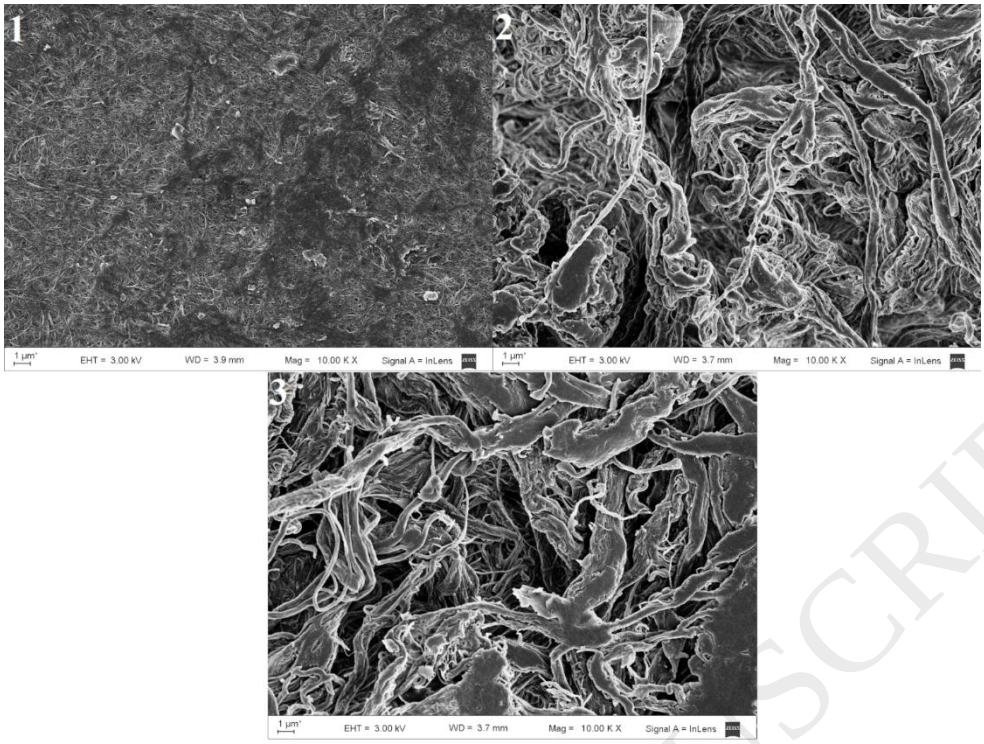

Fig. 3 FESEM images of native (1), alkalinized (2) and carboxymethylated BC (3)

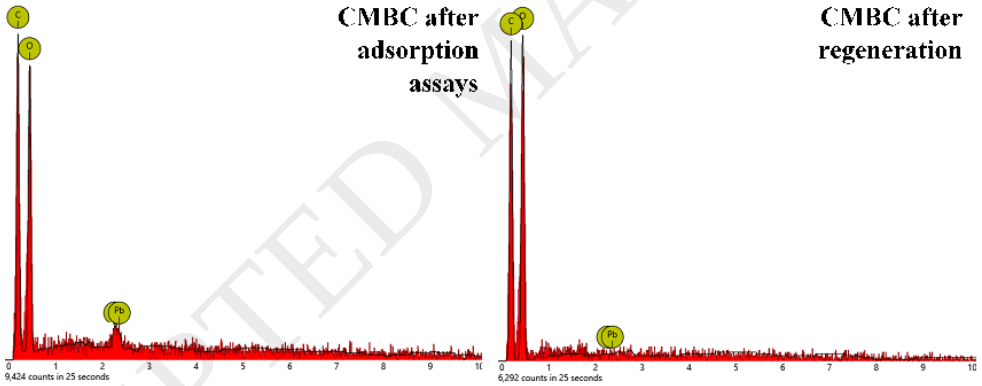

Fig. 4 EDS spectra of CMBC before and after regeneration

The effect of carboxymethylation on the crystallinity of BC was analyzed by X-ray diffraction (Fig. 5). The X-ray diffraction pattern of native BC showed signals characteristic of Cellulose I allomorph, with reflections of the cellulose lattice planes appearing at 2θ = 14.4° (101), 16.6° (10-1) and 22.6° (002), and a broad band at 34.4° assignable to the 040 plane. On the other hand, the diffractogram of BC was significantly altered by carboxymethylation, with reduced intensity in the Cellulose I

characteristic diffractions, and two new signals appearing at 2θ = 12.3° (shoulder) and 20.3°. These signals correspond to the 101 and 10-1 planes of Cellulose II respectively and account for the partial conversion of Cellulose I to Cellulose II allomorph induced by alkalinization [29].

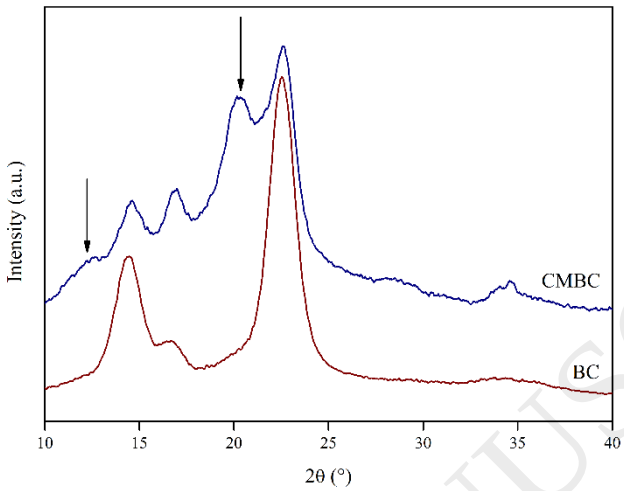

Fig. 5 X-ray diffraction patterns of BC and CMBC

3.2 Adsorption Studies

3.2.1 Adsorption kinetics studies

To know the extent of the use of the material, it is necessary to perform kinetic studies since, for certain specific applications, such as domestic use as a filter tap, a rapid adsorption kinetic is an indispensable requirement. The studies were performed at different temperatures and, as can be seen in Figure 6, the adsorption kinetic was fast in all cases and the equilibrium was reached at 60 minutes. Besides, a decrease in the capture rate was observed as the active sites of the CMBC began to be occupied until, upon saturation of the adsorbent, the curves reached a plateau.

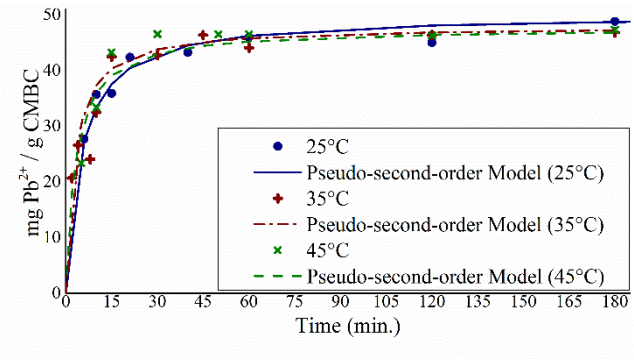

Fig. 6 Amount adsorbed of Pb^{2+} on CMBC at different times and temperatures.

Aiming to infer the controlling mechanism of the adsorption process, experimental data were adjusted to pseudo-first-order and pseudo-second-order models (Eq. 1 and 2, respectively), where q_t (mg g^{-1}) is the adsorption uptake at time t (min), q_e (mg g^{-1}) is the adsorption capacity and k_1 (min^{-1}) and k_2 (g mg^{-1} min^{-1}) are the kinetics rate constants [18,30].

$$\ln(q_e - q_t) = -k_1 t + \ln q_e \qquad \text{Eq. 1}$$

$$\frac{t}{q_t} = \frac{t}{q_e} + \frac{1}{k_2 {q_e}^2} \qquad \text{Eq. 2}$$

Results undoubtedly showed that, regardless of the temperature, the pseudo-second-order kinetic equation most appropriately described lead adsorption on CMBC (Table 1), suggesting that -as it was reported elsewhere-, the adsorption mechanism is kinetically controlled mainly by chemical interactions. The excellent concordance between the experimental data and those calculated by means of the pseudo-second-order kinetic equations is evidenced in Figure 6.

	Pseudo-first-order model			Pseudo-second-order model		
	k_1 (min^{-1})	q_e (mg g^{-1})	R^2	k_2 (g mg^{-1} min^{-1})	q_e (mg g^{-1})	R^2
25°C	0.033	19.6	0.8962	0.004	50.2	0.99995
35°C	0.05	18.5	0.8393	0.006	48.2	0.9984
45°C	0.005	16.1	0.0182	0.007	47.0	0.9986

Table 1 Comparison of the adsorption kinetic models

The pseudo-second-order constant and the temperature are related by the Arrhenius equation (Eq. 3), where k_2 is the pseudo-second-order rate constant, A is the Arrhenius factor, R is the gas constant, T is the temperature (K) and E_a is the activation energy (kJ mol^{-1}).

$$\ln k_2 = \ln A - \frac{E_a}{RT} \quad \text{Eq. 3}$$

Plotting *ln k2* against *1/T*, the activation energy value was obtained from the slope (Ea : 21.6 kJ mol^{-1} ; correlation coefficient (R^2) :0.9664) .

The magnitude of the activation energy may give an idea about the type of adsorption. In general, physical adsorption involves weak forces, and the activation energy is usually low (not more than 4.2 kJ mol^{-1}) [31]. In this case, the high activation energy value found for the adsorption of lead on CMBC is in agreement with the strong electrostatic interactions involved in this process.

3.2.2 Effect of pH

Figure 7 shows the strong pH dependence of lead adsorption on CMBC. This result was not suprising, considering that the degree of dissociation of weak acids (as the carboxymethyl group) is strongly dependent on pH.

Taking into account that the pka values of the carboxylic acids are around 5, below pH 4.8 more than 50 % of carboxyl groups remain protonated and cannot act as a cation exchanger. Contrary, at higher pH values, lead cations may be adsorbed to the surface

of CMBC through strong electrostatic interaction. On the other hand, as was expected, above pH 7 a precipitate was observed due to the formation of a water-insoluble lead hydroxide, as it was described elsewhere [32]. In summary, the CMBC lead adsorption capacity greatly increases at pH above 4.8; but, because of the metal solubility, the upper working pH value is limited to 7.

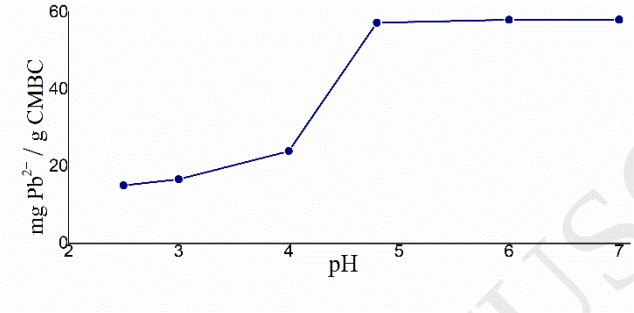

Fig. 7 Effect of pH on the removal of lead

3.2.3 Effect of ionic strength

Since the presence of high concentrations of other cations in the water can interfere with the lead capture capacity of the CMBC, the maximum capacity of lead adsorption of the resin as a function of the ionic strength was analyzed.

Figure 8 shows the effect of ionic strength on the uptake of lead by CMBC. As it can be seen, the uptake of lead decreases slowly as the ionic strength increases; an increase of two orders of magnitude of the ionic strength only reduced the maximum capture of lead by 27%. Therefore, it seems feasible to use this material in complex aqueous systems of high ionic strength.

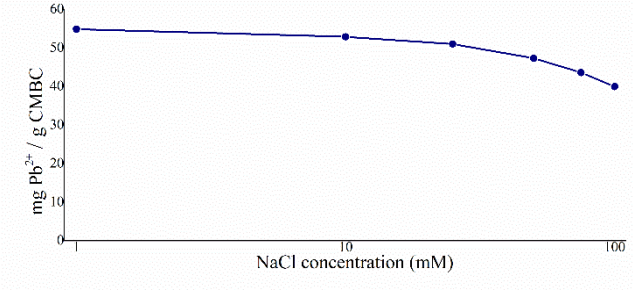

Fig. 8 Effect of ionic strength on the removal of lead

3.2.4 Adsorption isotherms

The capacity of an adsorbent can be described by equilibrium sorption isotherm, which is characterized by certain constants whose values express the surface properties and the affinity of the adsorbent [33]. Experimental isotherm data were fitted to different models of sorption isotherms: Langmuir, Freundlich, Dubinin-Radushkevich, and Frumkin. All the parameters of the models were evaluated by linear regression using Origin Pro 9.0.0 software. As can be seen in Table 2, the Langmuir equation gives the best fit of the collected data. Figure 9 shows experimental data against the curve obtained by the Langmuir model. On the other hand, the separation factor R_L indicates the type of the isotherm to be either unfavorable ($R_L>1$), linear ($R_L=1$), favorable ($0<R_L<1$) or irreversible ($R_L= 0$). In this case, the values of R_L factor were always between *0* and *1* for any value of initial concentration (C_0), indicating that adsorption of lead onto CMBC is favorable [34–36].

Model	Equation		Parameters			
			25°C	35°C	45°C	
Langmuir	$\frac{C_e}{q_e} = \frac{1}{bq_{max}} + \frac{C_e}{q_{max}}$ $R_L = \frac{1}{1 + bC_0}$	q_{max}	59.54	53.47	51.6	mg g^{-1}
		b	0.5146	0.3432	0.1213	L mg^{-1}
		R^2	0.9995	0.9948	0.9851	
Freundlich	$\log q_e = \log k_F + \frac{1}{n} \log C_e$	k_F	4.95	3.84	3.04	mg g^{-1}
		n	11.02	4.30	3.11	
		R^2	0.9503	0.7563	0.7814	
Dubinin–Radushkevich	$\ln q_e = \ln q_{D-R} - k_{D-R}\, \varepsilon^2$ $\varepsilon = RT \ln\left(1 + \frac{1}{C_e}\right)$ $E = \frac{1}{\sqrt{2k_{D-R}}}$	q D-R	55.6	51.1	46.1	mg g^{-1}
		k D-R	5.06 10^{-7}	2.9 10^{-6}	1.1 10^{-5}	mol^2 J^{-2}
		E	994.4	416.5	213.3	J mol^{-1}
		R^2	0.7033	0.7854	0.7621	
Frumkin	$\ln\left[\left(\frac{\theta}{1-\theta}\right)\frac{1}{C_e}\right] = \ln k + 2a\theta$ $\theta = \frac{q_e}{q_{max}}$	a	11.76	5.52	4.45	
		k	2.22 10^{-7}	1.229 10^{-2}	1.2 10^{-1}	L mg^{-1}
		R^2	0.969	0.9207	0.9488	

Table 2 Adsorption isotherm model parameters (q_e: equilibrium adsorption capacity; C_e: concentration of the balance solution; C_0: initial concentration of the solution)

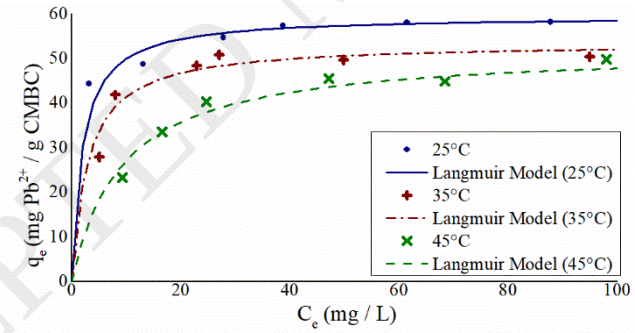

Fig. 9 Adsorption isotherm of lead on CMBC

In the Freundlich isotherm, the exponent *n* reflects the Pb^{+2} adsorption strength on CMBC. Taking into account that an adsorption process is considered favorable for *n>1* [37], the calculated values indicates a strong interaction between Pb^{2+} and CMBC.

Dubinin–Radushkevich isotherm is an empirical model generally applied to express the adsorption mechanism with a Gaussian energy distribution onto a heterogeneous surface

[38]. The model has been usually applied to distinguish between physical and chemical adsorption of metal ions according to the mean free energy (*E*) [39]. Regrettably, the correlation coefficient of this model was not satisfactory ($R^2 \approx 0.7$), so the mean free energy calculated was considered not representative of the process.

The Frumkin isotherm model has been specifically developed to take lateral interactions at the surface into account. The second term in the equation ($2a\theta$) reflects the extent of lateral interactions; if *a* is greater than *0* indicates attraction (as in the current case), while a negative value of *a* means repulsion [19]. The positive value of *a* can be explained by considering that, in addition to predominant ionic interactions, the adsorbent can form chelates with the lead cations through the CMBC hydroxyl groups.

The interaction between lead and the CMBC hydroxyl groups favors the adsorption process and represents an advantage of the developed material with respect to most cation-exchangers commercially available.

3.2.5 Thermodynamics parameters

Thermodynamics parameters ($\Delta G°$, $\Delta H°$ and $\Delta S°$) were calculated using the following equations [19,37]:

$$K_c = \frac{q_e}{C_e} \qquad \text{Eq. 4}$$

$$\ln K_c = \frac{-\Delta G°}{RT} \qquad \text{Eq. 5}$$

$$\ln K_c = \frac{\Delta S°}{R} - \frac{\Delta H°}{RT} \qquad \text{Eq. 6}$$

Where *T* is the temperature in Kelvin, *R* is the gas constant and K_c is the equilibrium constant. $\Delta H°$ and $\Delta S°$ were obtained from the slope and intercept of linear Van't Hoff plots of $ln\ K_c$ versus $1/T$. The results as well as the correlation coefficient (R^2) are shown in Table 3.

T (K)	ΔG° (kJ/mol)	ΔH° (kJ/mol)	ΔS° (J/mol K)	R^2
298	-6.55	-68.08	-206.57	0.9995
308	-4.40			
318	-2.42			

Table 3 Thermodynamics parameters for the adsorption of lead on CMBC

The negative value of $\Delta S°$ indicates a decrease in the randomness of the interface and the negative values of $\Delta G°$ indicate the spontaneous nature of the adsorption process. Besides, the observed decreased in the CMBC adsorption capacity when the temperature increased (Fig. 9) is in accordance with an exothermic process, as it was confirmed by the negative value of $\Delta H°$. In addition, the high absolute value of the enthalpy ($|\Delta H°| > 40\ kJ/mol$) is consistent with an adsorption mechanism governed by chemical interactions [40,41].

3.3 Column experiment

3.3.1 Breakthrough curve

In order to obtain the characteristic parameters for fixed-bed systems, experiments using a column packed with CMBC under continuous flow were conducted. The performance of this experiment can be described in terms of time vs. effluent concentration (breakthrough curve).

Several simple mathematical models have been developed to predict the dynamic behavior of the column. Among them, Bohart-Adams, Clark and Modified Dose-Response models are recommended because of the usefulness of the designed parameters that they provide [42–46]. Thus, those models were used here to estimate and analyze the column adsorption performance. All the parameters of the models were evaluated by non-linear regression using Origin Pro 9.0.0 software. In order to evaluate

the goodness-of-fit of the equation to the experimental data, the correlation coefficient (R^2), as well as the residual root mean square error (*RMSE*) and the chi-square test (χ^2) are presented. Figure 10 shows the breakthrough curve obtained against the curves fitted with the different models. The parameters of the models calculated from the simulations are presented in Table 4.

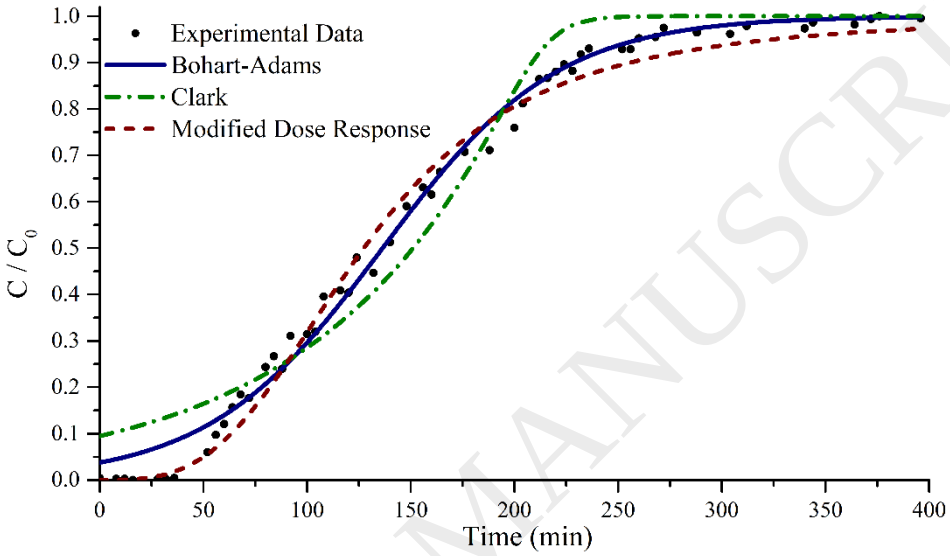

Fig. 10 Breakthrough curve

As illustrated in Figure 10 and Table 4, the Bohart-Adams and Modified Dose-Response models give the best fit to the experimental data, with slightly better correlation parameters for the first one.

The Clark model is based on the use of a mass-transfer concept in combination with the Freundlich isotherm [47]. As it was expected, considering that the Freundlich isotherm did not give an accurate correlation to experimental data, the Clark model does not represent satisfactorily the breakthrough curve herein obtained.

Model	Equation	Parameters		
Modified Dose	$\frac{C}{} = 1 - \frac{1}{}$	q_0	39.2	mg g^{-1}

Response		a	3.15	
		R^2	0.990	
		RMSE	0.071	
		χ^2	0.00137	
Bohart-Adams	$\frac{C}{C_0} = \frac{e^{k_{BA}C_0t}}{e^{k_{BA}N_0\frac{Z}{u}} - 1 + e^{k_{BA}C_0t}}$	k_{BA}	0.00365	L min^{-1} mg^{-1}
		N_0	2891.4	mg L^{-1}
		R^2	0.992	
		RMSE	0.056	
		χ^2	0.00108	
Clark	$\frac{C}{C_0} = \left(\frac{1}{Ae^{-rt} + 1}\right)^{\frac{1}{n-1}}$	A	1.74 10^{10}	
		r	0.11	min^{-1}
		R^2	0.962	
		RMSE	0.263	
		χ^2	0.00506	

Table 4 Breakthrough curve model parameters (*C*: lead concentration in the effluent; C_0: lead concentration in the influent; *Q*: flow rate; *t*: time; *x*: mass of CMBC; *Z*: bed depth; *u*: linear flow velocity; *n*: Freundlich constant)

3.3.2 Feasibility studies for CMBC reuse

Desorption studies were carried out with the aim to determine the technical feasibility of the reuse of CMBC, essential for an industrial application. Figure 11 shows the desorption curve obtained when HCl 6 mM (pH 2.2) was used as eluyent. As can be seen, almost 96 % of the retained lead was eluted in just 20 mL.

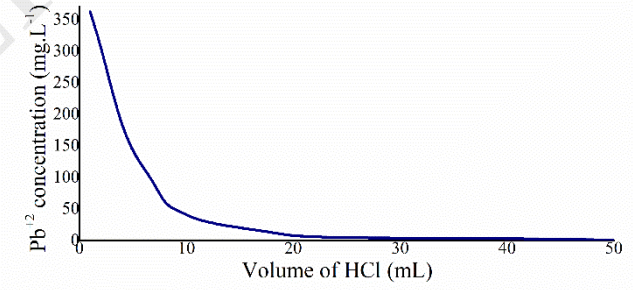

Fig. 11 Amount of Pb^{2+}desorbed from CMBC at different HCl (6 mM) volumes

Given that the possibility of reusing the adsorbent is one of the critical factors to consider in order to propose this methodology for lead removal at large scale, the

maximum number of regeneration cycles of the material before exhibiting a decrease in its retention efficiency was studied. The CMBC lifetime was over 50 adsorption/desorption cycles. As can be seen in Figure 12, the lead retention capacity of CMBC did not show significant variation along the 50 cycles investigated (Mean = 58 mg g^{-1}; SD =3.27 mg g^{-1}; RSD = 5.64%).

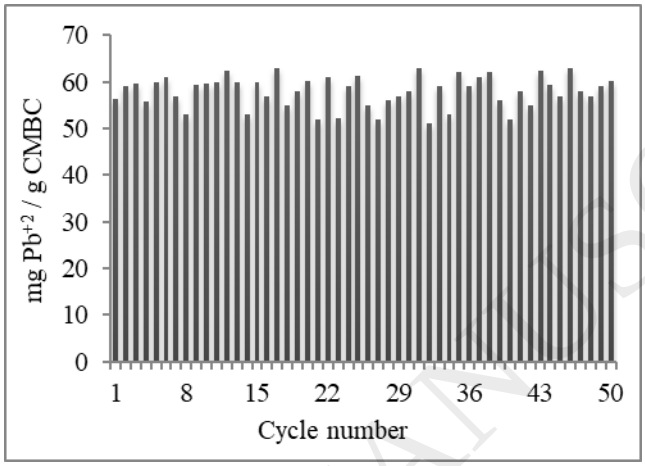

Fig. 12 Lead retention capacity of CMBC along the 50 cycles

X-ray analysis of the remaining sample was performed to analyze whether several uses had affected the structure of CMBC. As can be seen in Figure 13, except for some reduction in the intensity of the 10-1 plane of Cellulose II (2θ = 20.3°) relative to that of the 002 plane of Cellulose I (2θ = 22.6°), the diffractogram of CMBC after 50 cycles showed no significant changes with respect to original CMBC, with all the same signals present and similar crystallinity values calculated (i.e. close to 50% in both cases).

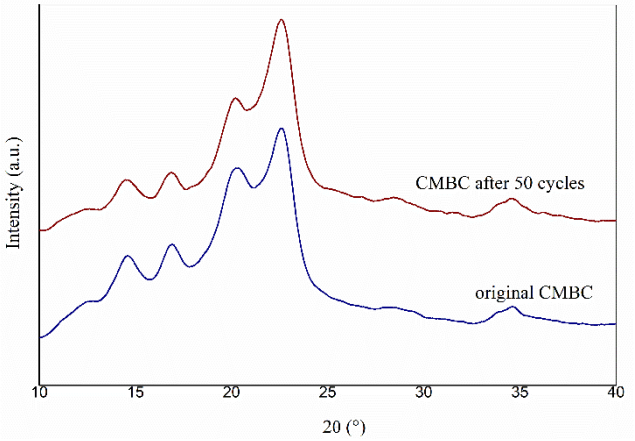

Fig. 13 X-ray diffraction patterns of original CMBC and the material after 50 adsorption/desorption cycles.

CONCLUSIONS

Water insoluble carboxymethylated bacterial cellulose (CMBC) was synthesized and its feasibility to be used as lead adsorbent was evaluated. CMBC showed good adsorption performance in the pH range of 4.8-7.0. The adsorption was fast following the pseudo-second-order kinetic model, which means that lead is adsorbed on CMBC predominantly by chemical interaction, as was confirmed by the thermodynamic parameters calculated for the process. In addition to predominant ionic interactions, the CMBC hydroxyl groups favor the adsorption process probably through chelation of lead cations. The experimental adsorption isotherm data and the breakthrough curve were well fitted with the Langmuir and Bohart-Adams models respectively.

Overall, the fact that the adsorption of lead was not significantly affected by ionic strength and CMBC remained unchanged after 50 regeneration cycles, suggest CMBC as a promising economic and environmentally friendly lead adsorbent for complex aqueous systems at large scale.

ACKNOWLEDGMENTS

The authors acknowledge Instituto Tecnológico de Buenos Aires for financial support. Ezequiel Rossi and Úrsula Montoya Rojo have fellowships from CONICET.

REFERENCES

[1] M.I. Errea, E. Rossi, S.N. Goyanes, N.B. D'Accorso, Chitosan: From Organic Pollutants to High-Value Polymeric Materials, in: S.N. Goyanes, N.B. D'Accorso (Eds.), Ind. Appl. Renew. Biomass Prod. Past, Present Futur., Springer International Publishing, Cham, 2017: pp. 251–264. doi:10.1007/978-3-319-61288-1_10.

[2] B. Liu, H. Qin, B. Zhang, T. Shi, Y. Cui, Enhanced oxidative stress by lead toxicity retards cell survival in primary thyroid cells, 2017. www.ijcem.com/ (accessed October 9, 2018).

[3] S.E. Schober, L.B. Mirel, B.I. Graubard, D.J. Brody, K.M. Flegal, Blood lead levels and death from all causes, cardiovascular disease, and cancer: results from the NHANES III mortality study., Environ. Health Perspect. 114 (2006) 1538–41. doi:10.1289/ehp.9123.

[4] M. Sajid, M. Younus, M.-R. Khan, A.A. Anjum, S. Ehtisham-ul-Haque, Effects of Experimental Lead Toxicity on Hematology and Biochemical Parameters in Lohi Sheep, Int. J. Agric. Biol. 19 (2017) 1409–1413.

[5] C. Hooper, X. Shi, Arsenic and lead in juice: apple, citrus, and apple-base, J. Environ. Health. 75 (2012) 14.

[6] M. Parmar, L.S. Thakur, Heavy metal Cu, Ni and Zn: toxicity, health hazards and their removal techniques by low cost adsorbents: a short overview, Int. J. Plant Anim. Environ. Sci. 3 (2013) 2231–4490.

[7] E. Rossi, M.I. Errea, M.M.F. de Cortalezzi, J. Stripeikis, Selective determination

of Cr (VI) by on-line solid phase extraction FI-SPE-FAAS using an ion exchanger resin as sorbent: an improvement treatment of the analytical signal, Microchem. J. 130 (2017) 88–92.

[8] L. Zhang, Y. Zeng, Z. Cheng, Removal of heavy metal ions using chitosan and modified chitosan: A review, J. Mol. Liq. 214 (2016) 175–191. doi:10.1016/j.molliq.2015.12.013.

[9] D.W. O'Connell, C. Birkinshaw, T.F. O'Dwyer, Heavy metal adsorbents prepared from the modification of cellulose: A review, Bioresour. Technol. 99 (2008) 6709–6724. doi:10.1016/j.biortech.2008.01.036.

[10] C.K. Jain, D.S. Malik, A.K. Yadav, Applicability of plant based biosorbents in the removal of heavy metals: a review, Environ. Process. 3 (2016) 495–523.

[11] Y. Jodra, F. Mijangos, Ion exchange selectivities of calcium alginate gels for heavy metals, Water Sci. Technol. 43 (2001) 237–244.

[12] X. Ma, X. Liu, D.P. Anderson, P.R. Chang, Modification of porous starch for the adsorption of heavy metal ions from aqueous solution, Food Chem. 181 (2015) 133–139. doi:10.1016/j.foodchem.2015.02.089.

[13] N. Chitpong, S.M. Husson, Polyacid functionalized cellulose nanofiber membranes for removal of heavy metals from impaired waters, J. Memb. Sci. 523 (2017) 418–429. doi:10.1016/J.MEMSCI.2016.10.020.

[14] V.K. Gupta, A. Nayak, S. Agarwal, Bioadsorbents for remediation of heavy metals: Current status and their future prospects, Environ. Eng. Res. 20 (2015) 1–18. doi:10.4491/eer.2015.018.

[15] J.N. Putro, S.P. Santoso, S. Ismadji, Y.-H. Ju, Investigation of heavy metal adsorption in binary system by nanocrystalline cellulose – Bentonite nanocomposite: Improvement on extended Langmuir isotherm model,

Microporous Mesoporous Mater. 246 (2017) 166–177. doi:10.1016/J.MICROMESO.2017.03.032.

[16] A. Jamshaid, A. Hamid, N. Muhammad, A. Naseer, M. Ghauri, J. Iqbal, S. Rafiq, N.S. Shah, Cellulose-based Materials for the Removal of Heavy Metals from Wastewater - An Overview, ChemBioEng Rev. 4 (2017) 240–256. doi:10.1002/cben.201700002.

[17] A. Casaburi, Ú. Montoya Rojo, P. Cerrutti, A. Vázquez, M.L. Foresti, Carboxymethyl cellulose with tailored degree of substitution obtained from bacterial cellulose, Food Hydrocoll. 75 (2018) 147–156. doi:https://doi.org/10.1016/j.foodhyd.2017.09.002.

[18] H. Ren, Z. Gao, D. Wu, J. Jiang, Y. Sun, C. Luo, Efficient Pb(II) removal using sodium alginate–carboxymethyl cellulose gel beads: Preparation, characterization, and adsorption mechanism, Carbohydr. Polym. 137 (2016) 402–409. doi:https://doi.org/10.1016/j.carbpol.2015.11.002.

[19] H. Demiral, İ. Demiral, F. Tümsek, B. Karabacakoğlu, Adsorption of chromium(VI) from aqueous solution by activated carbon derived from olive bagasse and applicability of different adsorption models, Chem. Eng. J. 144 (2008) 188–196. doi:https://doi.org/10.1016/j.cej.2008.01.020.

[20] C.S.T. Araújo, I.L.S. Almeida, H.C. Rezende, S.M.L.O. Marcionilio, J.J.L. Léon, T.N. de Matos, Elucidation of mechanism involved in adsorption of Pb(II) onto lobeira fruit (Solanum lycocarpum) using Langmuir, Freundlich and Temkin isotherms, Microchem. J. 137 (2018) 348–354. doi:10.1016/J.MICROC.2017.11.009.

[21] P. Cerrutti, P. Roldán, R.M. García, M.A. Galvagno, A. Vázquez, M.L. Foresti, Production of bacterial nanocellulose from wine industry residues: Importance of

fermentation time on pellicle characteristics, J. Appl. Polym. Sci. 133 (2016). doi:doi:10.1002/app.43109.

[22] S. Hestrin, M. Schramm, Synthesis of cellulose by Acetobacter xylinum. 2. Preparation of freeze-dried cells capable of polymerizing glucose to cellulose, Biochem. J. 58 (1954) 345–352. http://www.ncbi.nlm.nih.gov/pmc/articles/PMC1269899/.

[23] R.W. Eyler, E.D. Klug, F. Diephuis, Determination of degree of substitution of sodium carboxymethylcellulose, Anal. Chem. 19 (1947) 24–27.

[24] L.M. Ilharco, A.R. Garcia, J. Lopes da Silva, L.F. Vieira Ferreira, Infrared approach to the study of adsorption on cellulose: influence of cellulose crystallinity on the adsorption of benzophenone, Langmuir. 13 (1997) 4126–4132.

[25] A. Ashori, M. Babaee, M. Jonoobi, Y. Hamzeh, Solvent-free acetylation of cellulose nanofibers for improving compatibility and dispersion, Carbohydr. Polym. 102 (2014) 369–375. doi:https://doi.org/10.1016/j.carbpol.2013.11.067.

[26] C. Eyholzer, N. Bordeanu, F. Lopez-Suevos, D. Rentsch, T. Zimmermann, K. Oksman, Preparation and characterization of water-redispersible nanofibrillated cellulose in powder form, Cellulose. 17 (2010) 19–30.

[27] C.H. Ünlü, Carboxymethylcellulose from recycled newspaper in aqueous medium, Carbohydr. Polym. 97 (2013) 159–164.

[28] G. Dodi, D. Hritcu, M.I. Popa, Carboxymethylation of guar gum: synthesis and characterization, Cellul. Chem. Technol. 45 (2011) 171.

[29] E.N.J. Ford, S.K. Mendon, S.F. Thames, J.W. Rawlins, X-ray Diffraction of Cotton Treated with Neutralized Vegetable Oil-based Macromolecular Crosslinkers, J. Eng. Fabr. Fibers. 5 (2010).

[30] Y.S. Ho, G. McKay, Pseudo-second order model for sorption processes, Process Biochem. 34 (1999) 451–465. doi:https://doi.org/10.1016/S0032-9592(98)00112-5.

[31] E.I. Unuabonah, K.O. Adebowale, B.I. Olu-Owolabi, Kinetic and thermodynamic studies of the adsorption of lead (II) ions onto phosphate-modified kaolinite clay, J. Hazard. Mater. 144 (2007) 386–395. doi:10.1016/J.JHAZMAT.2006.10.046.

[32] H.T. Tran, N.D. Vu, M. Matsukawa, M. Okajima, T. Kaneko, K. Ohki, S. Yoshikawa, Heavy metal biosorption from aqueous solutions by algae inhabiting rice paddies in Vietnam, J. Environ. Chem. Eng. 4 (2016) 2529–2535. doi:https://doi.org/10.1016/j.jece.2016.04.038.

[33] L. Deng, Y. Su, H. Su, X. Wang, X. Zhu, Sorption and desorption of lead (II) from wastewater by green algae Cladophora fascicularis, J. Hazard. Mater. 143 (2007) 220–225. doi:https://doi.org/10.1016/j.jhazmat.2006.09.009.

[34] R. Dolphen, N. Sakkayawong, P. Thiravetyan, W. Nakbanpote, Adsorption of Reactive Red 141 from wastewater onto modified chitin, J. Hazard. Mater. 145 (2007) 250–255. doi:https://doi.org/10.1016/j.jhazmat.2006.11.026.

[35] J. Singh, N.S. Mishra, Uma, S. Banerjee, Y.C. Sharma, Comparative studies of physical characteristics of raw and modified sawdust for their use as adsorbents for removal of acid dye, BioResources. 6 (2011) 2732–2743.

[36] M. Khairy, R. Kamal, N.H. Amin, M.A. Mousa, Kinetics and isotherm studies of Remazol Red adsorption onto polyaniline/ cerium oxide nanocomposites, J. Basic Environ. Sci. 3 (2016) 123–132. http://jbesci.org/published/3.4.3.pdf (accessed October 9, 2018).

[37] A.A. Inyinbor, F.A. Adekola, G.A. Olatunji, Kinetics, isotherms and thermodynamic modeling of liquid phase adsorption of Rhodamine B dye onto

Raphia hookerie fruit epicarp, Water Resour. Ind. 15 (2016) 14–27. doi:https://doi.org/10.1016/j.wri.2016.06.001.

[38] M.M. Dubinin, The potential theory of adsorption of gases and vapors for adsorbents with energetically nonuniform surfaces, Chem. Rev. 60 (1960) 235–241.

[39] K.Y. Foo, B.H. Hameed, Insights into the modeling of adsorption isotherm systems, Chem. Eng. J. 156 (2010) 2–10. doi:https://doi.org/10.1016/j.cej.2009.09.013.

[40] S. Vasiliu, I. Bunia, S. Racovita, V. Neagu, Adsorption of cefotaxime sodium salt on polymer coated ion exchange resin microparticles: Kinetics, equilibrium and thermodynamic studies, Carbohydr. Polym. 85 (2011) 376–387. doi:10.1016/J.CARBPOL.2011.02.039.

[41] V.-P. Dinh, N.-C. Le, L.A. Tuyen, N.Q. Hung, V.-D. Nguyen, N.-T. Nguyen, Insight into adsorption mechanism of lead(II) from aqueous solution by chitosan loaded MnO2 nanoparticles, Mater. Chem. Phys. 207 (2018) 294–302. doi:10.1016/J.MATCHEMPHYS.2017.12.071.

[42] C.-G. Lee, J.-H. Kim, J.-K. Kang, S.-B. Kim, S.-J. Park, S.-H. Lee, J.-W. Choi, Comparative analysis of fixed-bed sorption models using phosphate breakthrough curves in slag filter media, Desalin. Water Treat. 55 (2015) 1795–1805. doi:10.1080/19443994.2014.930698.

[43] G.S. Bohart, E.Q. Adams, Some aspects of the behavior of charcoal with respect to chlorine, J. Am. Chem. Soc. 42 (1920) 523–544.

[44] G. Yan, T. Viraraghavan, M. Chen, A New Model for Heavy Metal Removal in a Biosorption Column, Adsorpt. Sci. Technol. 19 (2001) 25–43. doi:10.1260/0263617011493953.

[45] D. De, S. Santosha, V. Aniya, A. Sreeramoju, S. B., Assessing the applicability of an agro-industrial waste to Engineered Bio-char as a dynamic adsorbent for Fluoride Sorption, J. Environ. Chem. Eng. 6 (2018) 2998–3009. doi:10.1016/J.JECE.2018.04.021.

[46] M.L. Soto, A. Moure, H. Domínguez, J.C. Parajó, Batch and fixed bed column studies on phenolic adsorption from wine vinasses by polymeric resins, J. Food Eng. 209 (2017) 52–60. doi:10.1016/J.JFOODENG.2017.04.008.

[47] R.M. Clark, Evaluating the cost and performance of field-scale granular activated carbon systems, Environ. Sci. Technol. 21 (1987) 573–580.